Arc Movement of Intermediate-Frequency Vacuum Arc on TMF Contacts

Zhu Liying, Wu Jianwen, and Zhang Xueming

***Abstract*—This paper describes the arc behavior in the transverse-magnetic-field (TMF) contacts at intermediate frequency (400–800 Hz). With high-speed photography, three different arc modes were identified: expansion arc column, moving arc, and diffuse arc. In the expansion arc column mode, the arc column is immobile and the diameter of the arc column increases with the current. During this stage, the bright anode spots appear with high amplitude noise of arc voltage at high current. The expansion arc column mode plays an important role in the anode erosion. In the moving arc column mode, the average velocities were observed about 10–100 m/s, and the arc velocity increases with the increased frequency at the same current. The arc voltage expressed by arc current and frequency was obtained in this paper. The cross-section area of the arc column decreases with the increased frequency at the same current. The current density increases with the increased frequency at the certain current. Consequently, it is deduced that the arc velocity increases with the increased frequency at the same current. The mean power input concentrates in a smaller area at a higher frequency. It may be one of the reasons why the anode local melted.**

***Index Terms*—Arc appearance, arc mode, arc voltage, intermediate-frequency vacuum arc, transverse magnetic field (TMF).**

I. Introduction

With THE development of more or all electrical aircraft technology, the variable frequency power system has become the important development orientation for the aircraft in the future. The aviation area requires the new circuit breaker (CB) to replace the existing air CB. The vacuum CB has the advantageous characteristics: small volume, light weight, and large current-interrupting ability. It reaches the priority in the aviation field. However, the theory of intermediate-frequency vacuum arc needs further investigation. The present research of vacuum switch focuses on the frequency of 50 Hz/60 Hz, while there are few reports about vacuum CB operation from 360 to 800 Hz.

Manuscript received February 15, 2012; revised June 25, 2012, September 14, 2012, January 16, 2013, and March 27, 2013; accepted May 29, 2013. Date of publication July 29, 2013; date of current version September 19, 2013. This work was supported in part by Special Scientific and Research Funds for Doctoral Specialty of Institution of Higher Learning (200800060004), in part by the National Natural Science Foundation of China under Grant 50877002, and in part by the Innovation foundation of BUAA for Ph.D. graduates. Paper no. TPWRD-00155-2012.

Z. Liying and W. Jianwen are with the Department of Electrical Engineering, BeiHang University, Beijing 100191, China (e-mail: zhuliying0123@yahoo.com.cn; wujianwen@vip.sina.com).

Z. Xueming is with Changchun Institute of Optics, Fine Mechanics and Physics, Chinese Academy of Sciences, Changchun 130033, China.

Color versions of one or more of the figures in this paper are available online at http://ieeexplore.ieee.org.

Digital Object Identifier 10.1109/TPWRD.2013.2272590

It is well known that the evolution of arc mode has an influence on the current interruption ability. The arc appearance in experimental studies with cup-shaped transverse magnetic field (TMF) contacts has been described [1]. There are two kinds of typical arc modes: diffuse arc mode and constricted arc mode. When the interrupting current is a few kiloamperes, the arc is in the diffuse mode. The arc evolves to the constricted mode when the current exceeds a threshold value; in the constricted mode, the arc is more likely to cause the erosion of the anode [2].

The behavior of the vacuum arc in the TMF under line frequency is well described. Cheng and Poeffel [3], [4] studied the interaction of an immobile or creeping arc on a copper electrode. A large number of scholars studied the arc velocity and the relationship between the movement and the contact surface ablation [5], [6]. It is noted that the contact gap, contact material, and contact surface have a great influence on the arc velocity [7], [8]. Zalucki [9] investigated the vacuum arc modes, arc voltage, and frequency characteristics in 50-Hz and 900-Hz frequency with flat contacts. He presented qualitative correlations between the measured vacuum arc voltage and observed discharge modes.

Since there are few reports about the study on characteristics of the intermediate-frequency vacuum arc in the transverse magnetic field, the work presented in this paper focuses on the intermediate-frequency magnetic field arc modes and arc movement affected by frequency. First, according to the vacuum arc appearance, different forms of the arc mode are defined. Second, the arc velocities at different currents and frequencies are determined. Finally, the relationships between arc voltage and arc velocity were analyzed, and the reason why the arc velocities increase with increased frequency was also analyzed.

II. Experimental Setup

A single-frequency oscillating circuit was used to study the intermediate-frequency vacuum arc, as shown in Fig. 1. The detailed experimental operation is described as follows. At the start of the experiment, the charging voltage of capacitor C_2 is 220 V, and the charging voltage of capacitor C_1 is higher than that of capacitor C_2. Typical voltages across C_1 range from 155 V(5.6 kA) to 380 V(15.3 kA) at 400 Hz, and from 316 V(5.6 kA) to 848 V(15.3 kA) at 800 Hz. The vacuum interrupter VI is in closed position at this time. The trigger thyristor VT_2 is triggered first to ignite direct current, follows the contacts opening, and a vacuum arc is maintained with a small current of about 80 A until the contacts are fully open. Then triac VT_1 is triggered to inject intermediate-frequency current. The VT_2 is switched off due to negative voltage. The trigger signal of VT_1 lasts until

0885-8977 © 2013 EU

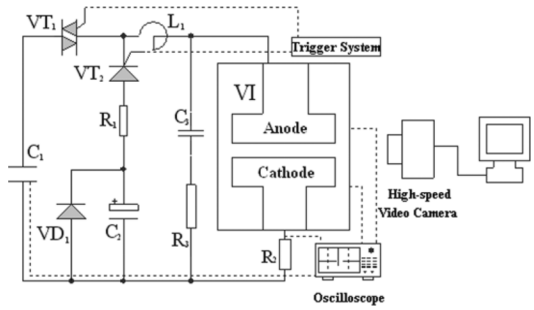

Fig. 1. Schematic diagram of the improved single-frequency oscillating circuit.

Fig. 2. Vacuum interrupters with TMF contacts.

the end of the experiment. By adjusting the capacitor C_1 and inductor L_1, 360 Hz–800 Hz current can be achieved. The amplitude of the first sinusoidal half-cycle current can change from 2 to 20 kA. Capacitor C_3 and resistor R_3 are used to adjust the rate of rise of recovery voltages (RRRV) parameters. The arc voltage was obtained from the voltage drop across the VI corrected for the induced voltage of the TMF contacts (L*dI/dt) and voltage drop caused by the resistance of the VI (R*I).

The experimental setup is different from that used in the actual CB. The contacts are first separated at low current, and only at the full contact gap is the high current switched on, and second, the current always starts at a low value, unlike in CBs that open at random points on the current cycle (including at current maximum). However, the experimental setup easily compares the results at different currents and frequencies, and it reduces the uncertainty of the experiment. The transition time between the initial constricted arc and the rotating or diffuse arc is significantly reduced compared to VI's in CBs. Even so, it has little impact on the arc modes, and it is more conducive to observe the arc appearance on the current arcing cycle.

The MotionProX3 high-speed video camera is used to record the arc shapes and the arc moving processes with the speed of 16 400 frames/s (60 μs/frame) and the exposure time of 5 μs. The arc voltage and current are recorded by the multichannel isolated oscilloscope. The specially designed sealed VI for intermediate frequency with cup-type TMF is utilized in the experimental system, as shown in Fig. 2. The electrode parameters are listed in Table I. The normally present metal shield of VI was removed in order to observe the vacuum-arc appearance, and this may have an effect on the arc motion. However, as the distance between the glass and contact is relatively long, it should have little impact on the arc motion.

TMF contacts are preferred above plain contacts. On plain contacts, the position of contact opening is badly defined which will lead to an undefined arc motion with the additional risk that the arc will come to a standstill at the contact edge. The TMF contacts create the same operating condition irrespective of the position of opening and will move the arc column in a reproducible rotational manner.

TABLE I
STRUCTURAL PARAMETERS OF THE VI

Contact diameter	Coil thickness	Highness of coil	Gap length	Contact thickness	Numbers of slot
66 mm	10 mm	18 mm	4 mm	2 mm	16
Contact material		Coil material		Air pressure	
CuCr50		Copper		$<10^{-4}$Pa	

TABLE II
INTERPRETATION OF THE PHOTOGRAPH PRESENTED IN FIG. 3

Times (ms)	Phase angle θ (°)	Arc characteristic	Arc current (kA)	Arc velocity (m/s)
0-0.24 (t_0-t_4)	0-35	A diffuse arc region near trigger with a single column. The single column remains stationary and the arc area increases.	0-7.1	-
0.24-0.96 (t_4-t_{16})	35-138	The diameter of single vacuum arc column changes little, and the arc column moving.	7.1-5.5	18
0.96-1.2 (t_{16}-t_{20})	138-172	The single moving column extinguished， no change is observed at the diffuse arc region.	5.5-1	-

III. RESULTS

A. Arc Mode

Vacuum arc appearance, arc voltage, and arc current were recorded at 400–800 Hz with a current peak value from 5–15 kA. The typical vacuum arc appearance, arc voltage, and arc current waveforms are shown in Fig. 3(a) and (b), respectively. The peak current and frequency are 10 kA and 400 Hz, respectively. The contact distance is 4 mm. Table II is the interpretation of the photograph presented in Fig. 3. The calculation method of the arc velocity in Table II is described in detail in Section III-E. The phase angle (θ) is used to compare arc-motion pictures captured at different frequencies, where $\theta = 360^\circ \times f \times t$.

According to the arc appearance, three stages of arc-mode evolution can be distinguished and are described in the following paragraphs.

1) Expansion arc column: As shown in Fig. 3(a), from t_0–t_4 (0°–35°), the arc has the following characteristics: The arc concentrates at the site of its initiation, and the arc diameter increases. The diffuse arc appears as a single arc column in the initial region. With increasing current, the single arc column diameter also gradually increases, while the arc remains immobile at the site of its initiation or starts creeping

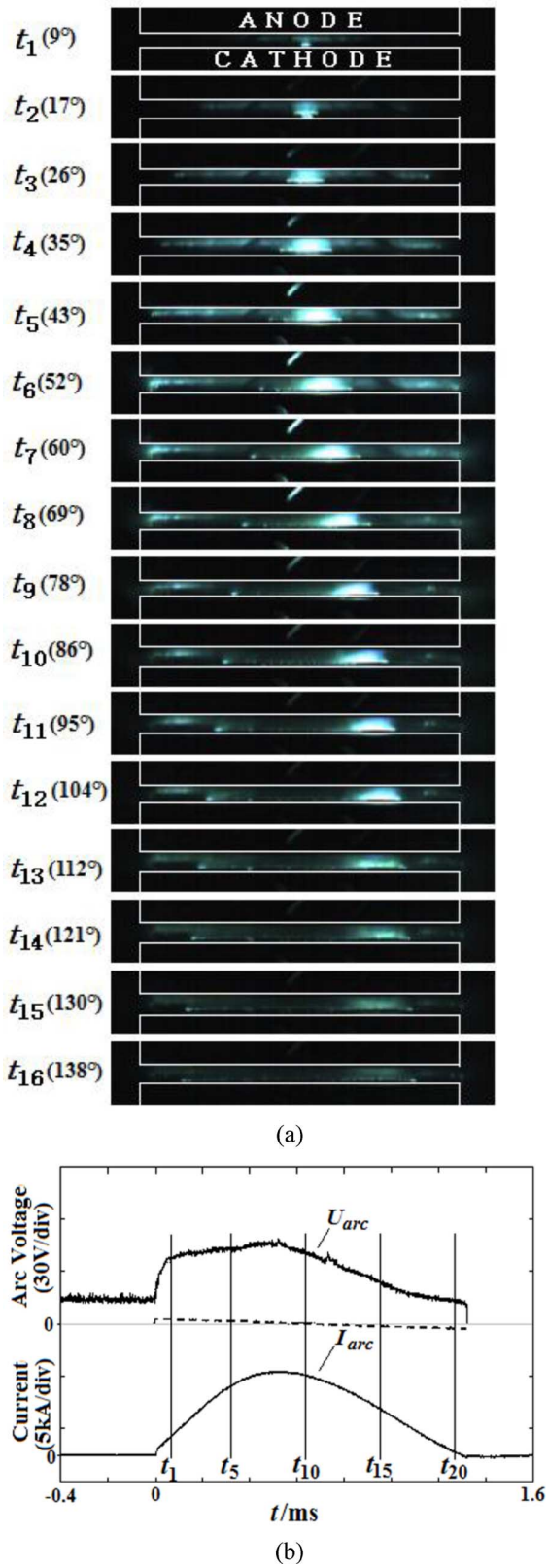

Fig. 3. Vacuum-arc appearance, arc voltage, and arc current at 400 Hz and 10-kA peak current. The dashed line represents arc voltage correction due to the inductance and resistance of the contact system: (a) arc appearances, (b) current, and arc voltage.

slowly (less than 3 m/s) using the definition of an immobile arc [7]. The arc voltage smoothly increases as shown in Fig. 3(b).

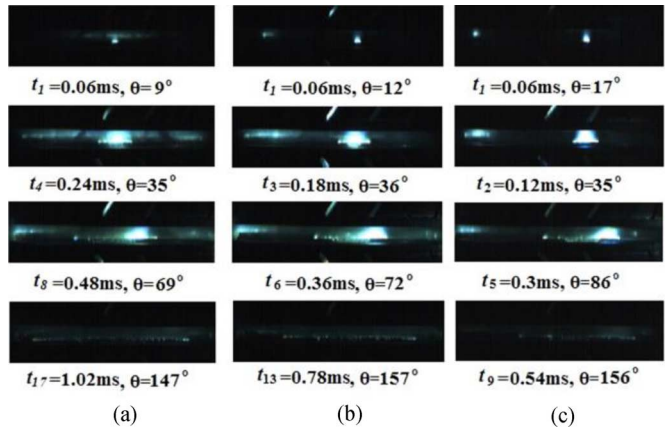

Fig. 4. Arc appearance at about 10-kA peak current and frequencies of 400, 560, and 800 Hz, respectively.

2) Moving arc column: At t_5–t_{16} (35°–138°), the arc moves smoothly with a velocity of 10–100 m/s. Generally, we observed that the arc did not move over a distance larger than half of the contact perimeter.
3) Diffuse arc: After t_{16} (138°), the bright arc disappears and spreads out into a diffuse arc. The diffuse arc [10] has the following characteristics: the diffuse interelectrode plasma, and distributed cathode spots. It can be further classified as a multicathode-spot vacuum arc. With the decreasing current, the cathode spots number and the arc light intensity reduces.

For frequencies higher than 400 Hz, the arc appearance has similar characteristics as with 400 Hz. Thus, from Fig. 4(b), we can see that the arc is an expansion arc column from t_1 (12°) to t_3 (36°). In this stage, we observe a single arc column expanding rapidly as the current increases. As shown in Fig. 4(b) t_6 (72°), the arc column moves at high velocity. At t_{13} (157°), the arc spreads out to a diffuse arc. The same characteristics were also shown in Fig. 4(c) at 800 Hz. At t_1 (17°) and t_2 (35°), the arc is an expansion arc column, and the arc moves at t_5 (86°), and diffuses at t_9 (156°). Furthermore, the cross-sectional area of the arc column decreases with the increase of frequency, as can be observed, according to t_4 [Fig. 4(a)] and t_2 [Fig. 4(c)].

With higher current ($>$10 kA), the arc modes also have approximately the same characteristic at different frequencies. However, the same characteristics of the arc column expansion stage depend on the current. Arc column expansion is an important arcing mode of the intermediate-frequency vacuum arc, and it has the following characteristics:

1) A single bright arc column whose diameter increases with current and decreases with frequency.
2) The arc remains immobile at the site of its initiation or starts creeping slowly (less than $<$3 m/s).
3) At currents higher than 13-kA peak current, the arc voltage has high amplitude noise which is accompanied by bright spots on the anode and the erosion spots on the anode contact surface.

Characteristics 1) and 2) occur simultaneously, and characteristic 3) depends on the current which only occurs at high current ($>$13-kA peak current), but it is accompanied by characteristics 1) and 2).

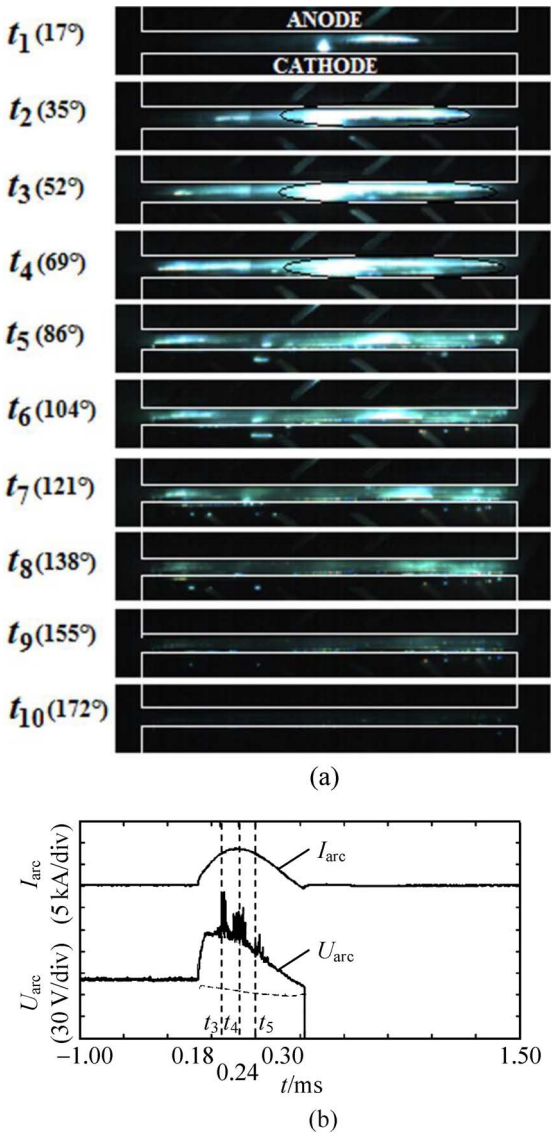

Fig. 5. Arc appearance, arc voltage, and arc current at 15.3-kA peak current, 800 Hz. The dashed line represents arc voltage correction due to the inductance and resistance of the contact system: (a) arc appearance and (b) arc current and voltage.

B. Anode Behavior

It is worth noting that the arc at high current (>13-kA peak value) has different characteristics in contrast to small current. First, the bright spots can be observed in the anode region, and sometimes the bright spots extend across the entire contact surface. Second, there are bright spots on the anode while the arc column remains immobile. However, during the arc column movement mode, the bright anode spots disappear.

Fig. 5(a) presents the detail process at high peak current at about 15.3 kA, 800 Hz. From t_1 (17°) to t_3 (52°) as the current increases during the expansion arc column mode, the arc column lights up in the initial arc position. Furthermore, bright spots near the anode can be observed at 15.3-kA peak current. This is different from the characteristic of 10-kA peak current. The bright spots near the anode disappear until t_5 (86°). The single arc column moves from t_4 (69°) to t_7 (121°). Then, after the disappearance of a single arc column, the arc is diffuse until it finally extinguishes. Fig. 5(b) shows the arc voltage and current waveforms when the peak current is 15.3 kA. As can be seen in Fig. 5(b), the arc voltage has high noise in t_3 (52°), t_4 (69°), and t_5 (86°). Based on the arc images, the arc voltage noise is correlated with bright spots near the anode.

Fig. 6. Anode contact after operations from 5.6-kA peak current to 15.3-kA peak current at 400, 475, 560, 650, and 800 Hz. The black line delimits the anode damage of the last test at 15.3-kA peak. (The inner and the outer diameters of the contacts are 46 and 66 mm, respectively.)

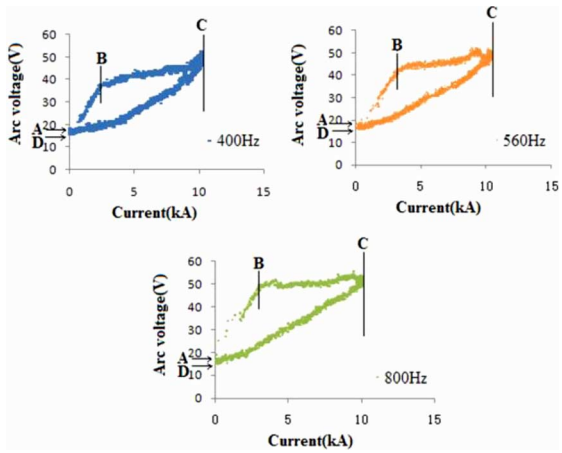

Fig. 7. Arc volt-ampere characteristics at about 10-kA peak current (400, 560, 800 Hz, respectively).

Fig. 6 is a still image of the anode surface showing the cumulated arc erosion of the anode surface for operations from 5.6- to 15.6-kA peak current at different frequencies (400, 475, 560, 650, and 800 Hz). The more serious erosion area marked by black ink is due to the last test at 15.3-kA peak current at 800 Hz. The marked position shows serious melting and erosion of the anode: the high bright area on the contact. This is attributed to the expansion arc column mode where the arc with high current does not move, which causes high energy concentration on a particularly small area.

C. Arc Voltage

The vacuum arc volt-ampere characteristics are dynamic. The volt-ampere characteristics can be divided into three stages [11]: the initial arcing stage, the transitional stage, and the current decline stage. Fig. 7 shows the vacuum arc volt-ampere characteristic curves at 400, 560, and 800 Hz for 10-kA peak current. Due to the random arc-initiation spot on contacts and the limitation of the sample rate of the oscilloscope, there is considerable uncertainty in the arc voltage data. However, the experimental

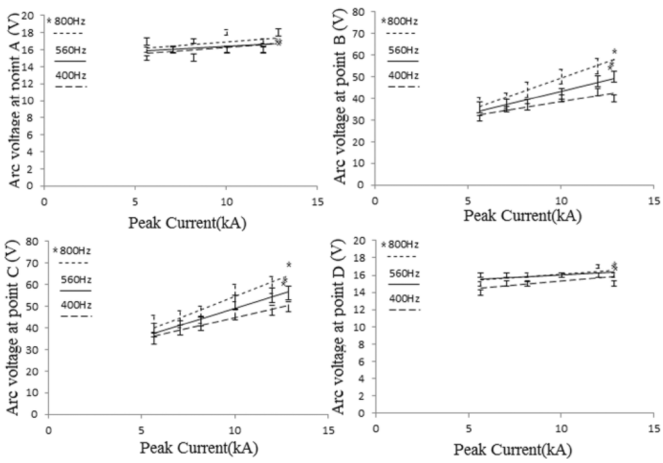

Fig. 8. Arc voltage at points A, B, C, and D.

results show the clear correlations between the arc voltage and frequency.

The volt-ampere characteristic curves at different frequencies 400 Hz, 560 Hz, 800 Hz, and 10-kA peak current show similar characteristics. It can be seen that the area surrounded by the arc volt-ampere characteristic curve increases with increased frequency. The volt-ampere characteristic curves can be characterized by the points A, B, C, and D. A is the starting point of the arc voltage, and corresponds to 0° phase angle; B is a turning point of the arc voltage which agrees to be less than 10°, C is the arc voltage corresponding to the peak arc current, and relates to 90° phase angle, D is the ending point of the arc voltage which corresponds to 180° phase angle. The arc voltages at points A, B, and C, D are measured at different frequencies and current values.

Fig. 8 displays arc voltage characteristic points A, B, C, and D at different frequencies and currents. The peak current is 5.6–15.3 kA, and the frequencies are 400, 560, and 800 Hz, respectively. The arc voltage at point A is almost constant, about 17 V. The initial arc voltage is determined by the cathode voltage drop in the cathode spot which is related only to contact material. For points A and D, the reproducibility is limited to the measurement accuracy of about 1 V.

The arc voltage at point B increased by 20 V at a frequency of 400 Hz and the peak current varies from 5.6 to 15.3 kA, and the arc voltage increased by 36 V at 800 Hz. The arc voltages at point B are closely related to the current amplitude and frequency. Both increasing current amplitude and frequency will cause the increase in arc voltage. The reproducibility is affected by the behavior of the arc with results in a precision of about 5 V. Fig. 8 illustrates that arc voltage at point B with current amplitude presenting the approximately linear relationship. The linear regression of arc voltage at point B and peak current is realized in Fig. 8.

As can be seen in Fig. 8, the arc voltages at point C also have a close relationship with current values and frequencies. The increase of either of them leads to higher arc voltage. As with point B, the arc voltage reproducibility is affected by the arc behavior. The linear regression of arc voltage at point C and peak current are also achieved and used to describe the relationship between them in Fig. 8.

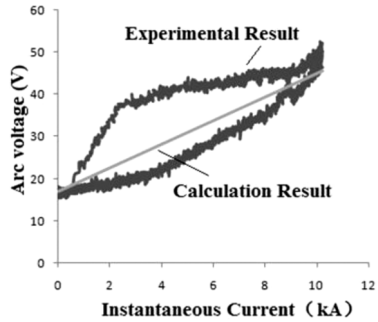

Fig. 9. Calculation result and experimental result of arc voltage at 400 Hz, 10-kA peak current.

The arc voltage at point D is near current zero. The arc voltages of point D lead to almost the same conclusion with point A, at about 16 V. It is appreciably lower than the arc voltages of point A. This is attributed to heating of the cathode after the arcing which results in the lower cathode voltage drop.

In [12], a correlation is presented between the arc voltage and current for rotating arcs at line frequency:

$$U_r = I_r R_r + U_0 \tag{1}$$

where U_r is the instantaneous arc voltage (in volts), and U_0 corresponds to the current-independent voltage drop at the cathode (in volts). I_r is the instantaneous arc current (in amperes) and $I_r R_r$ is the current-dependent voltage drop in the gap and at the anode (in volts).

A similar correlation is found here: the instantaneous arc voltage increases with instantaneous current and frequency. The instantaneous arc voltage has an approximately linear relationship with the frequency and the instantaneous current value, and the following relationship is obtained:

$$U_r = \mathrm{K}_0 f \cdot I_r + \mathrm{K}_1 I_r + \mathrm{U}_0 \tag{2}$$

where U_r is the instantaneous arc voltage (in volts), U_0 corresponds to the current-independent voltage drop (in volts). $\mathrm{K}_0 f \cdot I_\mathrm{r}$ and $\mathrm{K}_1 I_\mathrm{r}$ are associated with the voltage drop in the gap and at the anode (in volts), K_0, K_1 is constant, f is the frequency (in Hertz), and I_r is the instantaneous arc current (in amperes).

Typical K_0, K_1, and U_0 are calculated and K_0 is 0.004 mΩ/s, K_1 is 1.2 mΩ, and U_0 is 17 V. K_0, K_1, and U_0 are obtained by the bilinear least-squares method at 10-kA peak current with 400, 560, and 800 Hz. In Fig. 9, the experimental results were compared with the linear relation of (2) at 400 Hz, 10-kA peak current.

D. Mean Power Input in the Expansion Arc Column Stage

The power input can be calculated by the measured arc voltage and current. The mean power input stands for the average energy input in the contacts during the arcing time. It can be expressed as the following expression:

$$P = \frac{1}{t_r} W = \frac{1}{t_r} \int_0^{tr} \mathrm{u}_r i_r dt \approx \frac{1}{t_r} \sum_0^n \mathrm{U}_{rj} I_{rj} \Delta t \tag{3}$$

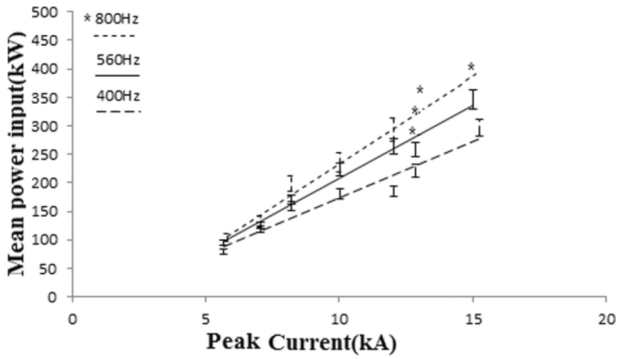

Fig. 10. Mean power input between the contacts at the expansion arc column stage.

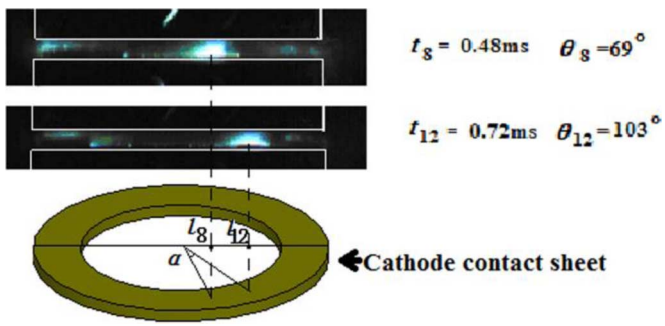

Fig. 11. Schematic diagram of the arc velocity calculation method.

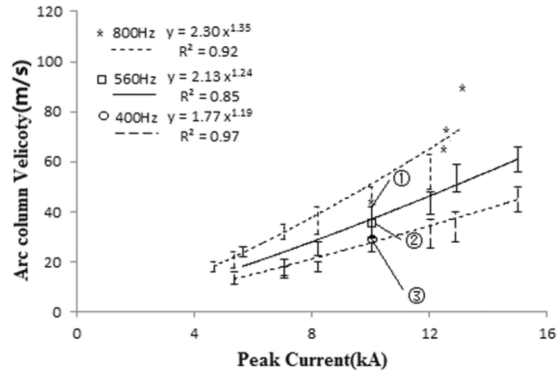

Fig. 12. Average velocity on phase angle 69°–103° at different frequencies (400, 560, 800 Hz).

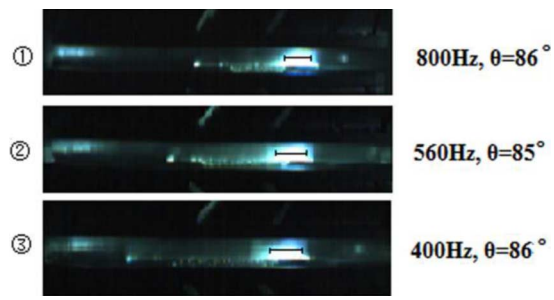

Fig. 13. Arc appearance corresponds to arc velocity remarked in Fig. 12 at about 86° phase angle.

where P is the mean power input (in watts), W is the arc energy (in joules), t_r is the arcing time, u_r is the instantaneous arc voltage (in volts), and i_r is the instantaneous arc current (in amperes). U_{rj} is the measured instantaneous arc voltage (in volts), I_{rj} is the measured arc current (in amperes), and Δt is the sampling interval of the digital oscilloscope used in this paper (100 ns).

In the expansion arc column stage, the arc remains immobile for a relatively long time, and the arc column diameter increases with the current. The mean power input of the expansion arc column stage at different frequencies was calculated, as shown in Fig. 10. The mean power input between the contacts increases with the current amplitude and frequency.

E. Arc Column Velocity

The arc velocity calculation method is illustrated in Fig. 11. First, it is assumed that the arc moves along the center line of the contact ring (radius 28 mm). Second, the location of the arc was taken by the highest brightness point of the arc. As shown in Fig. 11, at the t_8 to t_{12} interval, the arc locations were determined as l_8 and l_{12}, respectively, and projected to the center line of the contact ring. The angle (α) of the arc position was obtained, which was used to calculate the distance of the arc motion. The average velocity $(v_{\rm arc})$ of the arc motion is the arc movement distance divided by the duration of the interval. The phase angle is applied to compare the velocity of arc column motion $(\theta = 360^\circ \times f \times t)$. When the phase angle is the same, the current is also same at different frequencies.

According to the aforementioned calculation method, the average velocities of the arc column at a given phase interval were calculated at peak current 5.6–15.3 kA with frequencies of 400, 560, and 800 Hz. In addition, the relationships between the increased current and frequency with the average velocities of the arc were also analyzed. Fig. 12 shows the average velocities of the arc at different currents and frequencies (400, 560, 800 Hz) on a phase angle range from 69° to 103°. The reproducibility is related to the feature of the contact surface and the location of the initial arcing. The method of exponential fit was used to fit the relationship between the arc column velocity and the peak current at different frequencies. The fitting curves show the relationships between the arc column velocities and the peak currents. In addition to visually depicting the trend in the data with a regression line, the equations of the regression lines at different frequencies were calculated as shown in Fig. 12. $\rm R^2$ (R-squared) was calculated and displayed in the graph to describe the fit which was expressed as a correlation coefficient. The closer $\rm R^2$ is to 1.00, the better the fit. The average velocity of the arc rises with the current as shown in Fig. 12. Furthermore, the average velocity of the arc at the same current also increases with increased frequency.

The arc appearance at about the 86° phase angle was displayed in Fig. 13. The arc appearance corresponds to the velocities at about 10-kA peak current which were remarked in Fig. 12. The center line of the arc column was chosen and remarked as the arc column radius. The voltage drop occurs in the cathode, the arc column, and the anode sheaths. The cathode voltage drop in the cathode spot is related only to contact material. The size of the anode region is more difficult to measure than the arc column region. Therefore, the center line of the arc

column was chosen as the arc column radius. The arc column radiuses were measured at about 86°, and were 4.9 mm (800 Hz), 5.6 mm (560 Hz), and 6.4 mm (400 Hz). The radius of the arc column decreases with the frequencies at the same phase angle.

IV. Discussion

Although the arc mode is subject to the influence of the contact structure, the basic characteristics of the arc mode are similar. The form of arc was observed also by Zalucki [9] in 50-Hz and 900-Hz frequency with flat contacts, and three groups of arc modes were observed for decreasing currents. Constricted arcs without or with a small number of autonomous cathode spots mentioned by Zalucki are consistent with the moving arc column modes as mentioned before. The difference of the arc modes is caused by different forms of contact structure at different frequencies. Falkingham and Cheng [13] indicated that the arc remained constricted even at very low contact gaps at the initial examination of the high-speed films taken of these contacts. Although the movement of the arc has not been discussed, the experimental results correspond to the expansion arc column mode. At line frequency, the arc immobility phenomenon was investigated under some special conditions. According to Kimura [14], the interrupting limit of the spiral contact is closely related to the duration of the immobility or slow arc period. He supposed that there was a possibility of melt spot formation caused by energy transfer during the slow arc period. If the slow arc period becomes longer, then the energy transfer to one spot is prolonged. Consequently, a melt spot was generated at the contact surface. There is no doubt that the expanding arc column will result in the concentration of energy input. Therefore, it is likely to cause the erosion on the cathode and the anode, which has the influence on the interruption performance of current.

The contact is overheated locally due to the arc immobility. This may lead to a higher surface temperature of the contact even at current-zero, adversely affecting current interruption. The overheating of the contact surface can be prevented by forced arc motion. It is evident that arc movement considerably influences the interruption performance of current.

The average velocities of arc are about 16–100 m/s as measured here, and they correspond to those reported [10], [15], [16] who studied TMF contacts, and the velocities of the arc were about tens to hundreds of meters per second. Under the experimental conditions: hollow cylindrical cup electrodes, contact gap of 5 mm, the 6.5×10^{-6} T/A transverse magnetic field, and 9.3-kA peak current, [10] found similar arc velocities in the direction of $\mathrm{J} \times \mathrm{B}$ of about 5–35 m/s [10].

This paper showed that the average velocity of the arc increases with increasing frequency. The arc velocity could be a function of the current density and magnetic-field strength, as follows [17]:

$$v_{\mathrm{arc}} = I^{5/6}\sqrt{j}\left[\left(\frac{b_r L h_{ev}}{m_N}\right)\frac{4}{(T_b - T_0)^2 kc\rho \cdot \beta^2}\right]^{1/3} \Big/ \sqrt{\pi} \tag{4}$$

where I is the interrupted current intensity, j is the current density, L is the arc length, and b_r is the magnetic-field density to current ratio at the arc position. The material constants $\mathrm{m_N}, \mathrm{k}, \rho, \mathrm{c}, \mathrm{h_{ev}}$ can be found in a constant table. The other terms from the relation (4) are considered to be constant. The arc speed is roughly proportional to the current I, and to the square root of current density.

We assumed that the arc is completely ionized, and the electrical resistivity of arc is the same at the same current with a different frequency from 400 to 800 Hz. According to

$$R_{\mathrm{arc}} = \rho_{\mathrm{arc}}(l/S) \tag{5}$$

where l is the length of arc column (contact gap) and l is 4 mm in this paper, ρ_{arc} is the electrical resistivity of the arc column, and R_{arc} is arc column resistance, and S is the cross-sectional area of the arc column.

As described in (1) and (2), the arc column resistance can be written as

$$R_{\mathrm{arc}} = K_0 f + \mathrm{K}_1. \tag{6}$$

As described in (2), (5), and (6), the arc voltage correlates with the current value and the current frequency. If we take these expressions together, the following expression can be taken as:

$$S = \frac{\rho l I}{K_0 f \cdot I + \mathrm{K}_1 I} = \frac{\rho l}{K_0 f + \mathrm{K}_1}. \tag{7}$$

The current density can be expressed as follows:

$$j = \frac{I}{S} = \frac{\mathrm{K}_0 f I + \mathrm{K}_1 I}{\rho l} \tag{8}$$

where j is the current density, and $\mathrm{K}_0, \mathrm{K}_1, f, I, \rho$ and l have the same definitions as those in (2) and (4).

According to (7), the cross-sectional area of the arc column decreases with increased frequency when the current is the constant. It is in agreement with the conclusion achieved from the experiment result in Fig. 13. As shown in (8), the current density increases with the increased frequency at the same current.

Substituting (8) into (4), the arc column velocity expressed by the current and frequency are simplified as follows:

$$v_{\mathrm{arc}} \sim I^{5/6}\frac{\sqrt{\mathrm{K}_0 f I + \mathrm{K}_1 I}}{\sqrt{\rho}\sqrt{l}}. \tag{9}$$

The velocity of the arc increases with increased frequency. According to the experiment results of Fig. 12, the exponentiation relationships between the current and arc motion are obtained. The fitting curves of the experimental data are consistent with (9), and the equations of the regression lines supported (9) in Fig. 12. Although the arc motion is random, which was affected by the contact surface and initial arcing position, (9) can still be used to estimate the relationship between the arc column velocity and frequency.

As described in Section III-D, the mean power input increases with the increased frequency in the expansion arc column stage. According to the aforementioned conclusion, the local melting of the anode surface occurs during the expansion arc column stage. The anode is heated by the increased instantaneous energy-input: therefore, the energy input during a shorter arcing

time enables the anode local melting [12]. As shown in Fig. 4, the arc has more constricted arc columns and enhancement current density at higher frequency. The mean power input concentrates in a smaller area at higher frequency. A smaller area of the anode surface is being heated at a higher frequency with a given current. This could be one of the reasons why the anode local melts at higher frequency.

V. Conclusion

In this paper, the arc behavior on TMF contacts at different currents and frequencies (400–800 Hz) has been studied, and three arc modes have been identified. In particular, anode behavior and arc column velocity are the focus of this study. The following conclusions have been drawn:

a) There are three arc modes: expansion arc column, moving arc column, and diffuse arc on TMF contacts at the intermediate frequency (400–800 Hz).
b) In the low-current condition, the expansion arc column mode plays an important role in the anode erosion in the intermediate-frequency vacuum arc. During the expansion arc column stage, bright anode spots appear with high-amplitude noise of arc voltage at high current. It is the main cause of the anode erosion.
c) The arc velocity increases with the frequency at the same current. Analysis suggests that this is due to the frequency-dependent arc diameter.
d) The arc voltage increases with arc current and frequency.

Acknowledgment

The authors would like to thank Dr. H. Schellekens for his help with the English redaction of this report. They would also like to thank the team of the High Voltage Department, China Electrical Power Research Institute, for their kind help with the high-speed observation of the vacuum arc.

References

[1] W. Haas and W. Hartmann, "Investigation of arc roots of constricted high current vacuum arcs," *IEEE Trans. Plasma Sci.*, vol. 27, no. 4, pp. 954–960, Aug. 1999.
[2] J. V. R. Heberlein and J. G. Gorman, "High current metal vapor arc column between separating electrodes," *IEEE Trans. Plasma Sci.*, vol. PS-8, no. 4, pp. 283–288, Dec. 1980.
[3] L. C. Cheng and B. Y. Wan, "Arc immobility and erosion phenomena in low pressure air," in *Proc. 15th Int. Conf. Elect. Contacts*, Aug. 1990, vol. 1, pp. 561–568, 1990.
[4] K. Poeffel, "Influence of the copper electrode surface on initial arc movement," *IEEE Trans. Plasma Sci.*, vol. PS-8, no. 4, pp. 443–448, Dec. 1980.
[5] D. Gentsch and W. Shang, "High-speed observations of arc modes and material erosion on RMF- and AMF-contact electrodes," *IEEE Trans. Plasma Sci.*, vol. 33, no. 5, pp. 1605–1610, Oct. 2005.
[6] R. L. Boxman, "High current vacuum arc column motion on rail electrodes," *J. Appl. Phys.*, vol. 48, pp. 1885–1889, 1977.
[7] H. Manhart, W. Rieder, and C. Veit, "Arc mobility on new and eroded Ag/CdO and Ag/SnO2 contacts," *IEEE Trans. Compon., Hybrids, Manuf. Technol.*, vol. 12, no. 1, pp. 48–57, Mar. 1989.
[8] J. W. McBride, "Arc root mobility during contact opening at high current," *IEEE Trans. Compon., Packag., Manuf. Technol.*, vol. 21, no. 1, pp. 61–67, Mar. 1998.
[9] Z. Zalucki, "Transition from constricted to diffuse vacuum arc modes during high," *IEEE Trans. Plasma Sci.*, vol. 27, no. 4, pp. 991–1000, Aug. 1999.
[10] R. L. Boxman, E. Gerby, and S. Goldsmith, "Behavior of a high current vacuum arc between hollow cylindrical electrodes in a radial magnetic field," *IEEE Trans. Plasma Sci.*, vol. PS-8, no. 4, pp. 308–313, Dec. 1980.
[11] Z. Liying, W. Jianwen, W. Jing, and S. Yanhua, "Behavior of intermediate-frequency vacuum arc under transverse magnetic field," *Discharges Elect. Insul. Vacuum*, vol. 2, pp. 289–292, 2010.
[12] J. Wang, J. Wu, and L. Zhu, "Arc behavior of intermediate-frequency vacuum arc on axial magnetic field contacts," *IEEE Trans. Plasma Sci.*, vol. 39, no. 6, pt. 1, pp. 1336–1343, Jun. 2011.
[13] Falkingham, L. T. Cheng, and Kam, "Experiments in high current switching using small contact gaps," in *Proc. 17th Int. Symp. Discharges Elect. Insul. Vacuum*, Jul. 21–26, 1996, vol. 1, pp. 345–350.
[14] T. Kimura, A. Sawada, K. Koyama, H. Koga, and T. Yano, "Influence of vacuum arc behavior on current interrupting limit of spiral contact," *Discharges Elect. Insul. Vacuum*, vol. 2, pp. 443–446, 2000.
[15] E. Dullni, "Motion of high-current vacuum arcs on spiral-type contacts," *IEEE Trans. Plasma Sci.*, vol. 17, no. 6, pp. 875–879, Dec. 1989.
[16] C. Wolf, M. Kurrat, M. Lindmayer, and D. Gentsch, "Arcing behavior on different TMF contacts at high-current interrupting operations," *IEEE Trans. Plasma Sci.*, vol. 39, no. 6, pt. 1, pp. 1284–1290, Jun. 2011.
[17] E. Dullni, E. Schade, and W. Shang, "Vacuum arcs driven by cross-magnetic fields (RMF)," *IEEE Trans. Plasma Sci.*, vol. 31, no. 5, pt. 1, pp. 902–908, Oct. 2003.

Zhu Liying was born in Hebei Province, China, on February 14, 1985. She received the B.S. degree in electrical engineering from Northwestern Polytechnical University, Xi'an, China, in 2007 and is currently pursuing the Ph.D. degree in philosophy in electrical engineering from BeiHang University, Beijing, China.

Her research interests include the interruption of vacuum arc and its theory.

Wu Jianwen was born in Hebei Province, China, on June 13, 1963. He received the B.S. and M.S. degrees in electrical engineering from Shenyang University of Technology, Liaoning Province, China, in 1984 and 1987, respectively, and the Ph.D. degree in electrical engineering from Xi'an Jiaotong University, Xi'an, China, in 1995.

Currently, he is a Professor with the Department of Electrical Engineering and Deputy Dean of School of Automation Science and Electrical Engineering, BeiHang University, Beijing, China. He is primarily involved in the field of vacuum arc theory and its applications, power distribution automation systems, and power electronics.

Zhang Xueming was born in Hubei Province, China, on April 29, 1964. He received the B.S. degree in the application of electronic technology from the Changchun Institute of Optics, Fine Mechanics, Changchun, China, in 1987.

Currently, he is a Researcher with the Changchun Institute of Optics, Fine Mechanics and Physics, Chinese Academy of Sciences, Changchun. His research interests include aviation imaging and measurement techniques.